A Compact Third-Order 5 GHz Bandpass Filter with Enhanced Stopband Characteristics in Ultra Thin Organic Substrate

Seunghyun Hwang, Sunghwan Min, Hunter Chan, Venky Sundaram, and Madhavan Swaminathan

School of Electrical and Computer Engineering
Georgia Institute of Technology, Atlanta GA

***Abstract* — A lumped-element bandpass filter based on new RXP ultra-thin organic technology with enhanced stopband rejections is proposed in this paper. The design is based on a third-order capacitively-coupled resonator circuit with unique resonator and ground inductor. For demonstration of the proposed circuit and RXP technology, a 5 GHz bandpass filter has been implemented in a four-metal layer 0.191 mm thin RXP substrate. The measured results have a good agreement with the simulation and show that insertion loss is less than 1.24 dB with larger than 1 GHz bandwidth and sharp rejections at both low and high stopband.**

***Index Terms* — Filter, lumped-element, multilayer, RXP, SoP, WLAN.**

I. Introduction

Wireless communication systems have been dramatically evolved with innovative integration technologies such as system-on-chip, system-in-package, and system-on-package (SoP) [1]. Among these innovative system integration technologies, SoP has advantages in high RF performance as well as high integration capabilities [2] while SoP challenges excellent electrical performances as well as miniaturization size requirements. In order to satisfy these very demanding challenges, a dielectric material plays an important role. Therefore, an ultra-thin organic low-K dielectrics called RXP (RXP1: dielectric constant of 3.39 and loss tangent of 0.0038, RXP4: dielectric constant of 3.01 and loss tangent of 0.0043 at 5 GHz) have been developed and characterized [3], [4].

Microwave filter is an essential element in the wireless communication systems, and the bandpass filter (BPF) has the most important task in a wireless transceiver to suppress unwanted frequency signals including harmonic, image and intermodulation signals. In [5], a LTCC BPF designed for 5.5 GHz was presented, which has 1.1 dB insertion loss with larger than 1 GHz bandwidth. In [6], a second-order LTCC BPF for 5 GHz wireless application was presented with 1.4 dB insertion loss and 300 MHz bandwidth. Despite of LTCC good filter performances, its overall thickness does not meet the demanding size requirement.

In this paper, a new BPF in RXP dielectric material for 5 GHz wireless application is presented. The 0.191mm thin, more than four times thinner than LTCC, BPF is designed for a wide bandwidth (>1 GHz) with a considerably low insertion loss (<1.24 dB). Sharp rejections at both low and high stopband are obtained from a proposed BPF schematic, which creates multiple finite transmission zeros. In addition, a novel embedded capacitor called stitched capacitor has been used to avoid an unsymmetrical design that comes from the conventional parallel-plate capacitor layout. The total size of the filter is 2.6 x 2.2 x 0.191 mm^3, which is about five times smaller than LTCC filter (3.3 x 2 x 0.8 mm^3) [5]. To the author's best knowledge, this is the first demonstration of BPF design from the proposed circuit schematic on RXP material.

II. Filter Design

A. Circuit Topology

The major specification for the filter design is a sharp roll-off (rejection) response at the stopband because the stopband characteristics are a prime factor in determining the isolation between the transmitter and receiver in the wireless module. The sharp roll-off can be achieved by using a higher order filter topology, but the overall size is also increased. To efficiently improve the stopband characteristics without the size trade-off, transmission zeros can be added at a desired stopband. Fig. 1 shows a lumped-element circuit topology that can be used as a third-order BPF design for an enhanced stopband characteristic.

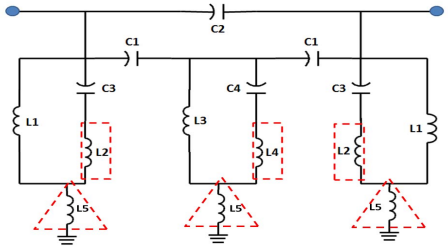

Fig. 1. Proposed third-order BPF schematic.

The circuit topology in Fig. 1 without the square and triangle areas has been known for producing two transmission zeros [7]; it used a second-order coupled resonator BPF in parallel with a feedback capacitor (*C2*) and magnetic coupling between inductors, which

introduce finite transmission zeros to the low and high stopband.

Instead of having the magnetic coupling between inductors, the additional elements (*L2, L4, L5*) can introduce multiple transmission zeros as shown in Fig. 2, which show the effect from those additional elements.

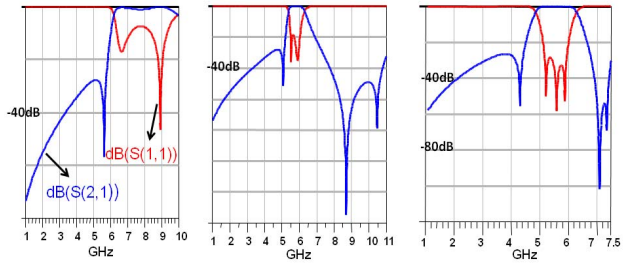

(a) (b) (c)

Fig. 2. BPF responses. (a) Without additional elements. (b) With L2 and L4. (c) With L2, L4, and L5.

Fig. 2(a) shows the response without any additional elements and magnetic coupling. It is clear to see that the bandwidth is very wide without rejection at the high stopband. After series inductors (*L2* and *L4*) are included, Fig. 2(b) shows two transmission zeros for the high stopband. These additional inductors, in fact, are necessary for the multilayer organic BPF layout design. For instance, a capacitor can be readily realized by using parallel-plates on two different layers. To make a connection from the capacitor to other elements such as an inductor, the layout requires an interconnect or via that can be represented as an inductance in microwave frequencies. Therefore, *L2* and *L4* can be used as design parameters, which do not affect the size of the layout.

Likewise, *L5* can be used as a ground connection through a ground layer. In a multilayer layout, there must be at least one ground connection from the BPF layout to the ground layer. As shown in Fig. 2(c), the rejection response from Fig. 2(b) is dramatically improved by adding the *L5*. It is important to note that the lumped-elements values in Fig. 2 have not been changed, but only *L2*, *L4*, and *L5* are added to improve the filter response.

The series inductors are related to the high stopband transmission zeros, which can be calculated by

$$L2 = \frac{1}{(2\pi f_{tz1})^2 \cdot C3} \tag{1}$$

$$L4 = \frac{1}{(2\pi f_{tz2})^2} \cdot \frac{C1 + C4}{C1 \cdot C4} - L3 \tag{2}$$

where f_{tz1} is the first high stopband transmission zero and f_{tz2} is the second transmission zero frequencies. After including series inductors, the ground inductor can be obtained by

$$L5 = \left| \frac{L1 \cdot [1 - (2\pi f_{tz3})^2 \cdot L2 \cdot C3]}{1 - (2\pi f_{tz3})^2 C3 \cdot (L1 + L2)} \right| \tag{3}$$

where f_{tz3} is a desire high stopband rejection frequency. In addition, the location behavior of additional transmission zeros can be easily observed by tuning *L2*, *L4*, and *L5* in commercial circuit simulator [8].

Although the design equations for individual circuit elements can be approximately obtained from a classical microwave design guide [9], it must be noted that the basic circuit topology is difficult to model the actual physical layout in the multilayer design because of unpredicted parasitic and coupling between elements in the layout. Hence, the usage of full-wave electromagnetic (EM) simulator is necessary to examine the parasitic effect of via and coupling between lumped-elements due to the close proximity within the structure. However, the proposed filter schematic can serve as a major design guide to verify individual elements behavior before EM solver is used for the physical layout, which reduces design-cycle significantly.

B. Physical Layout Design

To demonstrate the performance of the proposed circuit schematic and RXP material, a 5 GHz BPF is designed by the circuit schematic shown in Fig. 1 and is realized by RXP material. First, each lumped-element values except the additional elements are calculated by the classical microwave design equation [9]. Then, additional elements are included and optimized so that the response has the sharpest roll-off at the stopband while it maintains low insertion loss and wide bandwidth. The circuit element values in Fig. 1 are *L1*=0.31 nH, *L2*=0.34 nH, *L3*=0.34 nH, *L4*=0.55 nH, *L5*=0.37 nH, *C1*=0.41 pF, *C2*=0.21 pF, *C3*=0.99 pF, *C4*=0.76 pF. After obtaining all of lumped-element values, each element is replaced by a corresponding layout. With RXP technology, the unloaded quality factor for the inductor is around 100 at 5 GHz. Fig. 3 shows a physical layout of the organic BPF embedded in a four-metal layer RXP substrate, and the layer structure is shown in Fig. 4.

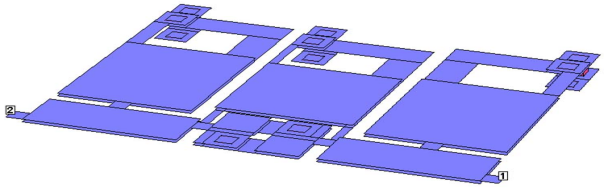

Fig. 3. Physical layout of 5 GHz third-order BPF.

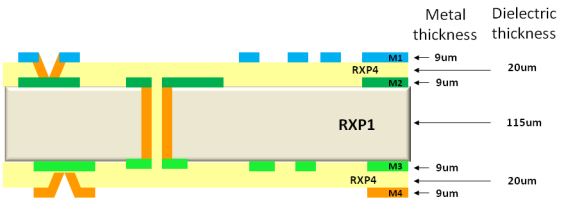

Fig. 4. Layer structure of RXP organic material.

Metal layers 1, 2, and 3 (M1, M2, and M3) are used to layout the components while metal layer 4 mainly serves as the ground plane. The first completed layout is further optimized to have better performances because parasitic effects and coupling from the close proximity between elements affect the designed performance from the circuit simulator. To reduce the design-cycle time, the proposed schematic in Fig. 1 is used to examine behaviors of lumped-elements so that only corresponding inductors or capacitors for better performances are allowed to be modified in the layout. The final layout shows 0.88 dB insertion loss at 5.5 GHz with 1.35 GHz 3 dB bandwidth and more than 25 dB rejections within 400 MHz from the passband as shown in Fig. 5.

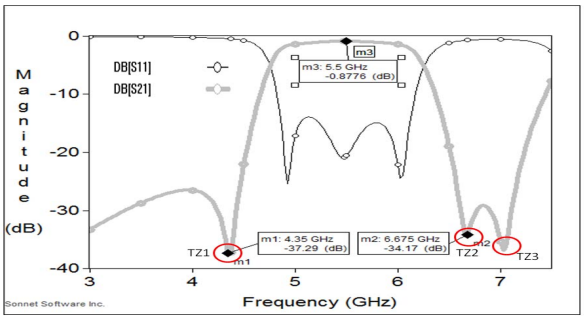

Fig. 5. 5GHz BPF response in EM simulator.

As shown in Fig. 5, the designed BPF has multiple transmission zeros; the low stopband transmission zero (TZ1) occurs around 4.4 GHz while high stopband transmission zeros (TZ2, TZ3) occur around 7 GHz to enhance both low and high stopband characteristics.

III. Stitched Capacitor

In addition to the proposed topology, the capacitor in the layout is designed by a stitched (3D inter-digitated) capacitor. The basic idea of the stitched capacitor is to combine the advantages of a 3D parallel-plate capacitor with a 2D inter-digitated capacitor. The design flow of the capacitor is to segment the parallel-plate capacitor into arbitrary shape and number of sections and then to stitch the segmented sections using vias to meet the required capacitance. The main advantages of this capacitor layout are an easy access to input/output ports and symmetrical shunt capacitance parasitics. The stitched capacitors providing the same parasitic shunt capacitance at input/output ports from the same layer is shown in the right side of Fig. 6.

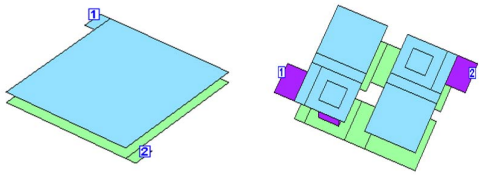

Fig. 6. Parallel-plate capacitor and stitched capacitor.

In the parallel-plate capacitor shown in the left side of Fig. 6, the input and output ports (port1, port2) are always located in the different layer, which makes uneven shunt capacitance parasitics and unsymmetrical layouts. For instance, the feedback capacitor (*C2*) in Fig. 1 is connected to port1 and port2 of BPF. If the feedback capacitor is designed by the parallel-plate capacitor, the interconnect from the port2 of the feedback capacitor requires a via. Since only one side of the feedback capacitor has a via inductance, the entire design becomes unsymmetrical. Although the stitched capacitor requires two vias, the feedback capacitor made by the stitched capacitor maintains the symmetry. Hence, it contributes to improve the performance especially in the insertion loss.

Furthermore, the desirable shunt parasitics can also be obtained by controlling the bottom surface. Since both input/output ports can be accessed from the same metal layer, surface mountable devices can be directly mounted on the exposed top metal surface. For instance, stitched capacitors can be tuned and optimized by mounting additional capacitors, and resonators can be realized by mounting inductor. Finally, tunable BPF can be realized by mounting inductors and capacitors horizontally and vertically. Moreover, it provides vertical routing flexibility by mounting interconnects such as bonding wires and bumps.

IV. Experimental Results

The proposed RXP BPF has been fabricated by Package Research Center (PRC) at *Georgia Institute of Technology*. The overall size of the filter is 2.6 x 2.2 x 0.191 mm^3, which shows the high integration capability of the ultra-thin RXP substrate. The fabricated prototype based on the physical layout in Fig. 3 is shown in Fig. 7.

The measurement was carried out using short-open-load-thru (SOLT) calibration by Agilent PNA 8363B with Cascade GSG-500 air coplanar probes. The measurement result from 1 to 10 GHz is shown in Fig. 8, and both measured and simulated frequency responses are shown in Fig. 9.

According to the measurement, the measured BPF response has an excellent correlation with the simulation. The prototype BPF exhibits a center frequency of 5.3 GHz and a 3 dB bandwidth of 1.4 GHz. The return loss is low 20 dB and the insertion loss is 1.235 dB at the center frequency, which is quite low considering the loss tangent of RXP is almost 2 times higher than LTCC. Furthermore, better than 25 dB rejections within 400 MHz from the passband is achieved, which is ideal for rejecting unwanted signals. The small discrepancies in the model-to-hardware may come from production variations in fabrication, but the performance is not deteriorated, showing the proposed design and RXP material are effective in the filter design.

V. Conclusion

A compact third-order 5 GHz BPF in RXP substrate was successfully designed, fabricated, and measured. The proposed BPF circuit topology for producing multiple transmission zeros has been verified through the design and measurement. The measurement showed good agreement with the simulation, and had less than 1.24 dB insertion loss with more than 1 GHz bandwidth while it maintained high rejections at both low and high stopband. This paper also presented a stitched capacitor, which has been used for making a completely symmetrical design. Based on the results, RXP filter can be used in RF applications since they have a high integration capability as well as high performances.

Acknowledgment

The authors would like to thank Embedded Actives and Passives (EMAP) consortium members for supporting this work.

References

[1] R. Tummala, and M. Swaminathan, *Introduction to System-on-Package (SOP)*: McGraw-Hill, 2008.

[2] M. Swaminathan, A. Bavisi, W. Yun *et al.*, "Design and fabrication of integrated RF modules in liquid crystalline polymer (LCP) substrates," in Industrial Electronics Society, 2005. IECON 2005. 31st Annual Conference of IEEE, 2005, pp. 6.

[3] S. Hwang, M. Swaminathan, and V. Venkatakrishnan, "Extraction of material properties for low-K and low-loss dielectrics using cavity resonator and efficient finite difference solver up to 40GHz," in Electrical Design of Advanced Packaging and Systems Symposium (EDAPS), Seoul, S. Korea, Dec. 2008, pp. 53-56.

[4] V. Sundaram, H. Chan, F. Liu *et al.*, "Super high density two metal layer ultra-thin organic substrates for next generation system-on-package (SOP), SiP and ultra-fine pitch flip-chip packages," in Pan Pacific Microelectronics Symposium, Hawaii, 2009.

[5] W. Yu, B. Yuan, and H. Sun, "A compact quasi-lumped LTCC band pass filter for C-band wireless application," in ICMMT, 2008, pp. 1488-1490.

[6] K.-B. Lee, and J.-Y. Lee, "5.2GHz band 2nd-order band-pass filter using LTCC multi-layer technology," in APMC, 2005, pp. 4.

[7] L. K. Yeung, and K.-L. Wu, "A compact second-order LTCC bandpass filter with two finite transmission zeros," *IEEE Transactions on Microwave Theory and Techniques,* vol. 51, no. 2, pp. 337-341, Feb. 2003.

[8] Agilent, *ADS (Advanced Design System) 2008*.

[9] G. L. Matthaei, L. Young, and E. M. T. Jones, *Microwave filters impedance matching networks and coupling structures*, pp. 355-410: New York:McGraw-Hill, 1980.

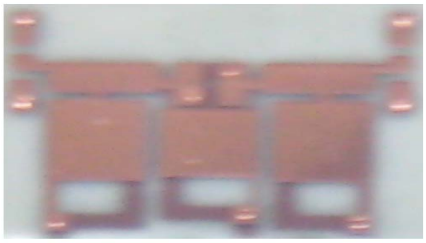

Fig. 7. Fabricated RXP 5 GHz BPF.

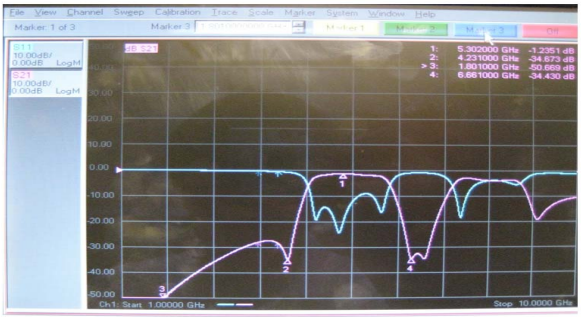

Fig. 8. Measured frequency response from VNA.

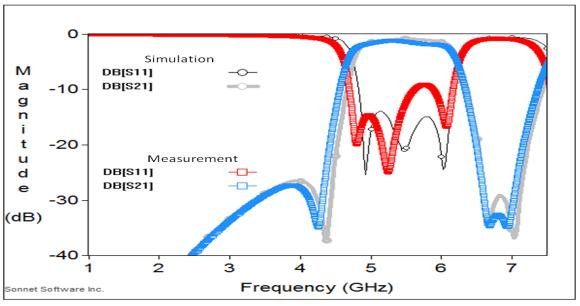

Fig. 9. Model-to-hardware